Enhancing Heliostat Calibration on Low Data by Fusing Robotic Rigid Body Kinematics with Neural Networks

Max Pargmann[a,1,*], Moritz Leibauer[b,1], Vincent Nettelroth[b], Daniel Maldonado Quinto[a], Robert Pitz-Paal[a]

[a]*German Aerospace Center (DLR), Institute of Solar Research, Linder Höhe, D-51147 Köln, Germany*
[b]*Synhelion Germany GmbH, Am Brainergy Park 1, 52428 Jülich, Germany*

Abstract

Solar tower power plants rely on precise calibrations of their heliostats for efficient operation. Open-loop calibration procedures are the most common type due to their cost-effectiveness. Two main approaches to these algorithms exist: geometry-based robotic kinematics and neural network-based models. While the former is reliable and requires little data, it only yields moderate accuracy. The latter, however, promises higher accuracies but is data-hungry and unreliable. In this study, we propose a 2-layer coarse-to-fine hybrid model that combines the strengths of both approaches. Our model uses a rigid-body model for prealignment, then phases in a neural network disturbance model through a regularization sweep. This approach ensures that the prediction accuracy is, in the worst-case, equivalent to that of the rigid-body model. Moreover, it helps to identify deficiencies that may have been overlooked by the physical approach. It especially is capable to compute deviation from the geometry models averaged optimum. For testing, we used real measurement data from daily heliostat calibration at the solar tower in Jülich. We also employed a training/validation data split for evaluation, which allows for a conservative performance assumption over the entire year. Our results demonstrate that the hybrid-model outperforms rigid-body models starting from the first measurement, achieving a top performance below 0.7 milliradians. In conclusion, our proposed hybrid model provides a cost effective in-situ solution for heliostat calibration with highest accuracies on low data in solar tower power plants for all open loop calibration methods.

Keywords: Mechanical Engineering, Renewable Resources, Robotics, Concentrating solar tower power, Heliostat aiming, Artificial intelligence, Neural Networks

1. Introduction

The use of solar tower power plants has been gaining momentum as a promising source of clean and renewable energy as well as solar fuels. These plants use an array of mirrors, known as heliostats, to reflect and concentrate sunlight onto a central receiver, where the energy is then converted into electricity. The sun tracking accuracy of these heliostats is essential for maximizing the energy output and overall efficiency of the power plant. For keeping the accuracy high, the heliostats have to be calibrated regularly. However, due to cost constraints affecting especially the material and component quality of the heliostats, the required accuracy is difficult to achieve.

The Camera-Target Method (Stone, 1986) is the standard method for heliostat calibration due to its high accuracy, reliability and relatively low cost implementation. During calibration, each heliostat is moved individually from the receiver to a white calibration target nearby the receiver. A camera is positioned to have a clear view of the target and captures focal spot images from various sun positions throughout the days. These images are used to determine the heliostats' deviations in position and orientation via a rigid-body regression model. Traditionally, physical-mathematical models have been used to determine the optimal positioning.

New approaches are being developed to improve the tracking accuracy of heliostats through the use of neural networks. These approaches require large datasets for training but deliver far better accuracies compared to common physical models (Sarr et al. (2023); Pargmann et al. (2021)). However, since the data set delivered by the Camera-Target Method is rather small per heliostat, the use of neural networks is very limited. Furthermore, even if the data set is sufficient, they are not as reliable as their physical counterpart.

We here present a 2-layer coarse-to-fine hybrid model, which uses a proven to be reliable geometric model as a prealignment and then phases in a neural network disturbance model over a regularization sweep. This ensures, that the model performs in the worst case as good as the geometric model, but can profit from small dynamic variations, provided by the neural network. For testing we use real measurement data from the daily heliostat calibration carried out at the solar tower in Jülich. We use a k-Nearest Neighbor (k-NN) training/validation data split to give a

*Corresponding author
Email address: max.pargmann@dlr.de (Max Pargmann)
[1]These authors contributed equally to this work.

conservative performance estimation of our models over the year.

2. Related Work

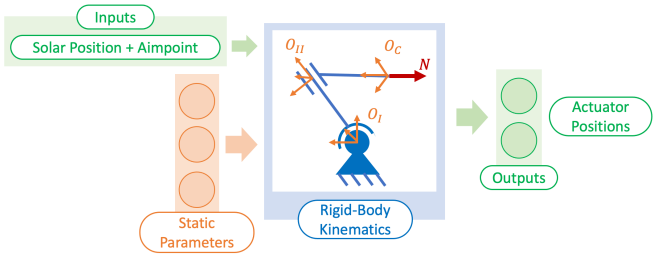

Figure 1: Rigid Body Alignment Model

Historically, the approach first suggested by Baheti and Scott (1980) and visualized in Figure 1 is the most implemented one (Stone, 1986; Chen et al., 2004, 2006; Chong et al., 2009; Guo et al., 2010; Khalsa et al., 2010; Guo et al., 2013; Smith and Ho, 2014; Freeman et al., 2017; Grigoriev et al., 2020, 2021). The heliostat alignment model is derived from an investigation of the heliostat's kinematics and actuator geometry. Baheti and Scott (1980) introduced six deficiencies: three rotations around the east, north and up axis, one gear ratio deficiency for each of the two actuators and a bias due to measurement errors of the elevation angle. Stone (1986) extended the number of deficiency corrections to eight. Smith and Ho (2014) described these eight parameters as "pedestal tilt about the east axis", "pedestal tilt about the north axis", "azimuthal reference bias", "elevation reference bias", "azimuth linear error", "elevation linear error", "drive-axis non-orthogonality" and "boresight error". Freeman et al. (2017) first applied Denavit-Hartenberg notation and thus extended coordinates to alignment modelling. However, in most cases the description of the heliostat is reduced to static errors, because the underlying optimization algorithm computes an average best fit over the entire behavior range.

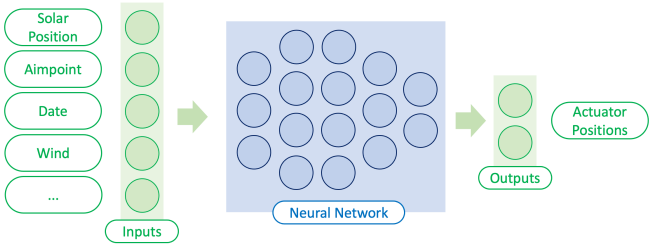

Figure 2: Sketch of a neural network for alignment prediction.

The more general approach, visualized in Figure 2, is using a neural network to predict the alignment. This approach can learn modelling a heliostat's complete alignment behavior, including dynamic impacts such as wind

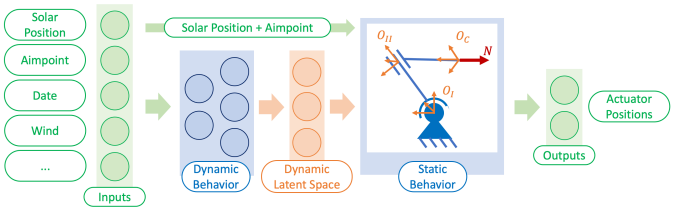

Figure 3: Combination of Rigid-Body-Kinematics and Dynamic Deviations

and thus promises high prediction accuracies. Furthermore, no prior analysis of the heliostat's kinematics is required. Possible implementations were thus pursued by Lee and Park (2010); Guangyu and Zhongkun (2017); AL-Rousan et al. (2020). A major drawback to this approach is the prediction's complexity. This leads to high amounts of required training data to successfully modify the networks parametrization. Nonetheless, advancements in techniques such as transfer learning, data augmentation, and active learning have enabled researchers to achieve impressive results with smaller data sets. In a previous publication we (Pargmann et al. (2021)) suggested pre-training the neural networks on simulated data, to pre-configure the neurons' linkage and thus reduce the amount of required training data. The method achieved very high accuracies but still needed 300 data points per training. Using more modern neural network architectures, the amount of needed data could already be reduced to 60 data points (Sarr et al., 2023). Comparing the size of data sets and achieved accuracy across various publications is challenging due to the significant influence of the data set on the results (Pargmann et al. (2023)). However, a trend towards attaining higher accuracies with deep learning approaches with less data is observed in recent developments.

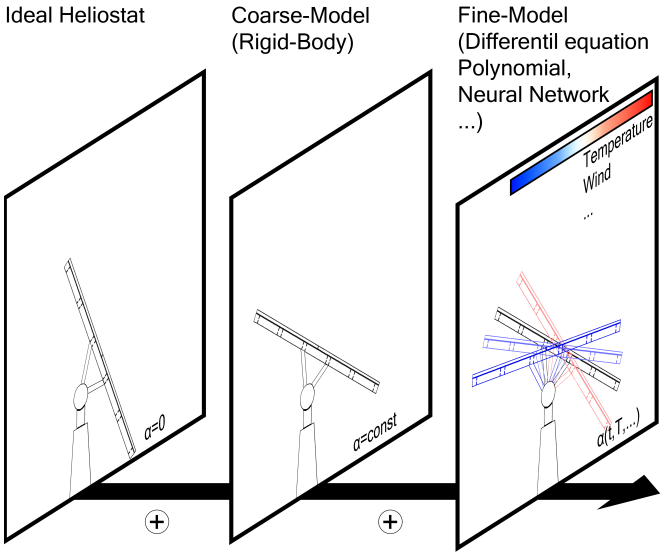

Figure 4: The layers of our propoased heliostat model. At the first layer, the heliostat is decribed by an ideal rigid-body model. In the second layer, the rigid-body model is trained using 28 optimizable parameters. The trained parameters are then saved and used as reference points for the the last layer, which adds dynamic calculated perturbations

3. Theoretical Outline

3.1. Comprehensive Heliostat Model

For our results, we use a universal heliostat model (first presented here Pargmann et al. (2023)) as the basis. It is a rigid-body kinematic system, designed along the lines of robotic manipulators, with each joint serving as the origin of a new coordinate system. These coordinate systems can be rotated and translated along three axes but are interdependent as part of a chain, resulting in six degrees of freedom. Modifications to a coordinate system at a higher level in the chain impact all of its child systems. This methodology allows us to not only compute the alignment of a heliostat in global coordinates based on its actuator configuration but also derive the actuator configuration from a given target alignment using the inverse principle of coordinate systems. The model is able to describe every bi-axial heliostat using a maximum of 28 (partly interdependant) parameters. In the following it will be referred to as the *coarse-model*, due to its limitations of computing average optima over for the entire heliostat behavior.

The second layer, *the fine-model*, serves as a disturbance model that introduces dynamic deficiencies. A schematic visualization is given in Figure 3. Each parameter that can be optimized in the first layer is assigned an additional function in the fine-model. If the coarse-model provides constant values for these parameters, the fine-model uses them as a reference point and only predicts deviations from these values. However, if there are no constant values given, the fine model predicts all optimizable parameters, by learning the static average deviation as well as dynamic

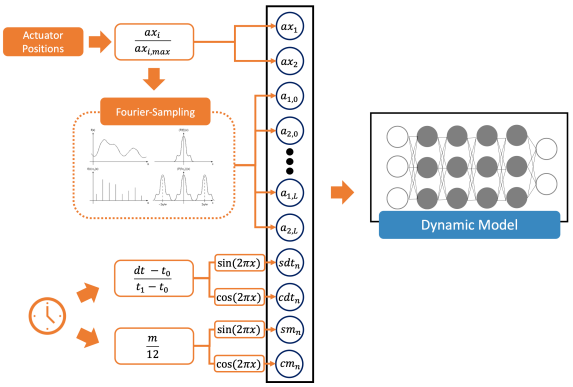

Figure 5: schematic drawing of the used inputs for the neural network. All inputs are encoded using fourier feature mapping.

local deviations. Technically any function e.g. polynomials, differential equations, or neural networks can be used for this purpose on any of the 28 free parameter. As long as the chosen disturbance model is (partly) differentiable these functions can be optimized as well. The method is schematically drawn in Figure 4.

3.2. kNN Training-Evalutation Splitting

In a previous publication (Pargmann et al. (2023)), we employed a Training/ Evaluation/ Test split for heliostat calibration datasets based on the distance between a measurement point and its k Nearest Neighbors (kNN with $k = 1, 2, 3$) with respect to the sun position in Euler angles (Azimuth, Elevation). To create these splits, the full dataset was sorted by the kNN distance. The test set was populated with 30 data points, using measurements with the greatest distance to their neighbors. The validation dataset used further 20 data points, still sorted by the kNN distance. All remaining data was used for training. If the dataset size was restricted, measurements with the smallest kNN were excluded from training. All accuracies presented later refer to the test dataset and are strictly correlated with their kNN distance to the training dataset. This type of Training-Test Splitting removes valuable information from training. Training with a different split, such as a randomly ordered split, will likely result in significantly better accuracies, due to the smaller distance to the validation and test data set. However, as noted in our earlier publication, this accuracy can be considered a conservative performance assumption, and it is not expected to fall short in daily operation.

3.3. Neural Network Architecture

Our Fine Model is represented by a simple multi-layer perceptron (MLP). The general architecture corresponds to a self normalizing neural network (SNN). The basic principle behind SNNs is that the prediction by construction of the network, strives for a prediction mean value around zero with a standard distribution value of one. While it is possible for a SNN to learn to exceed this prediction range,

all exceeding values experience a pull towards the targeted range of prediction. Thus, predictions can be bounded to a certain range without loosing the gradients. They can also be much deeper and thus solve more complex tasks than simple MLPs.

A neural network configuration of 14 hidden layers with two neurons per layer was found to yield good results. However, we did not employ any parameter exploration or optimization techniques; instead, we utilized the initial architecture that proved to be effective.

As (normalized) inputs we use the heliostat's orientation, as well as the month and time of the measurement. Inputs like environmental conditions are not further discussed as no data was available. Due to the periodic behavior of time and date, it holds two different types of information. The first type is its normalized duration Δt_n from a given date t_0, which can indicate the amount of wear on a system. The normalized duration can be derived by interpolating the current date t between an earliest date t_0 and latest date t_1 (ref. Equation 1). Then the normalized duration is encoded into a sine and cosine function.

$$\Delta t_n(t) = \frac{t - t_0}{t_1 - t_0} \tag{1}$$

The second type of information is the season, which can be shown as normalized month m_n that is constructed by dividing a data points' month m by twelve. This input can indicate seasonal biases. This could be corrections to the solar algorithm or environmental impacts, whereby the latter should be used as individual inputs (e.g. temperature) if available. Daily cycles are already encoded within the solar position and thus given through the heliostat's orientation.

The heliostat orientation can be extracted from the heliostat's actuator configuration. Therefore, a data point's actuator steps a_i are normalize to $a_{i,n}$ by dividing a_i by its maximum allowed value $a_{i,max}$ for each actuator i.

In addition the heliostat orientation is extended via Fourier feature mapping (Tancik et al., 2020). This approach was found to significantly improve a neural network's performance for low-dimensional regression tasks, where high-frequency features within the input data were not noticed by the network until explicitly been introduced as additional inputs. These additional inputs are obtained by splitting each input parameter's value into multiple inputs, one each for a different frequency band.

Lastly we use weight decay to regularize the neural network. Weight decay is a regularization technique that is used to prevent overfitting of the model during the training process. It involves adding a penalty term to the loss function that is proportional to the squared sum of the neural networks weights. The penalty term is multiplied by a hyperparameter, known as the weight decay coefficient, which controls the amount of regularization applied. Higher weight decay coefficient renders the neural network parameter space less complex.

4. Method

Our approach comprises a two-step process that utilizes a combination of a coarse and fine model. During the first step, the coarse model is solely pre-trained using the sun position, heliostat position, aimpoint, and measured position of the focal spot. This pre-training step is important as it establishes a firm starting point for the subsequent fine-tuning step. During the fine-tuning step, the fine-model is trained using additional inputs, such as the date of measurement.

After the training step, the fine model is trained and its outputs are added to the static parameters of the first layer, which is then used to predict accurate alignment. Similar to weight decay, pre-training helps to reduce the complexity of the parameter space. Moreover, due to pre-training, the weight decay now pulls the network's output towards well-working parameters instead of zero, thus binding the network to previously obtained knowledge.

The fine-model training is performed iteratively, beginning with high regularization to force the network to find solutions close to the coarse model. We can now gradually decrease the weight decay until it reaches zero and compare the test results to the coarse model results using the same test data. As we will see later, regularization is only required very infrequently as the two-layer system performs significantly better in most cases, even without regularization.

5. Datasets

In total, we gatherd 4 Datasets from 4 different Heliostats at the solar tower in Jülich in the time between Mai 2021 and October 2022. The Datasets contain between 191 and 477 Datapoints. The datasets where collected in daily operation. So no extra measurement campaign has taken place for this work has taken place. We cannot exclude that points were recorded outside the automated calibration routine. Especially for AJ23 this is very likely.

Table 1: Characterizing properties of the heliostat data sets.

Name	Position (East/North)	Time Range	Datapoints
AJ23	-54m/66m	6/21-10/22	477
AM35	-4m/80m	5/21-10/22	191
AM42	26m/80m	5/21-10/22	216
AM43	31m/80m	8/21-10/22	198

6. Proof of Concept at the Solar Tower in Jülich

First we want to evaluate the performance of our Hybrid-Model, by varying the amounts of applied training data. Our findings are presented in Fig. 6. The upper graph of the figure shows the accuracy of three different coarse models (Static 6, 14, and 20), as it is typical in the state

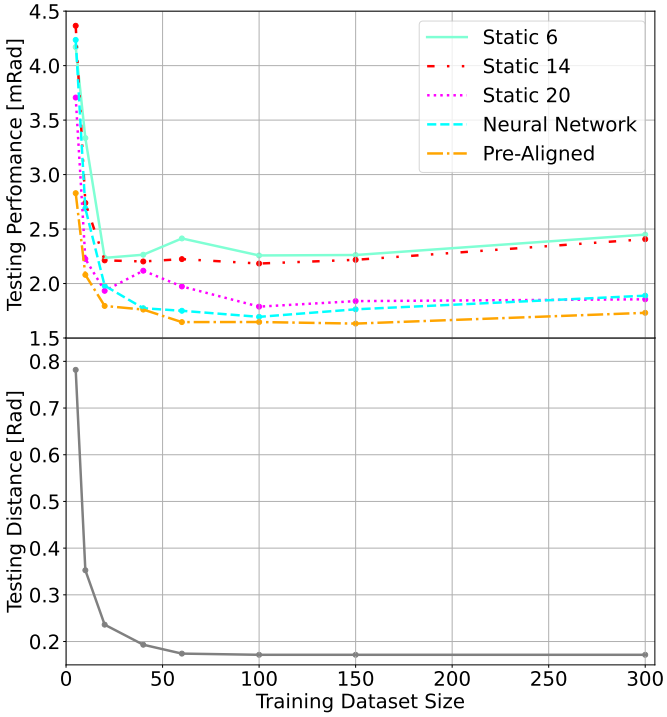

Figure 6: Comparison of different coarse models (*Static 6,14,20*), the fine model (*neural network*) and the hybrid model (*pre-alignment*) using the fine model together with the coarse model as a pre-alignment

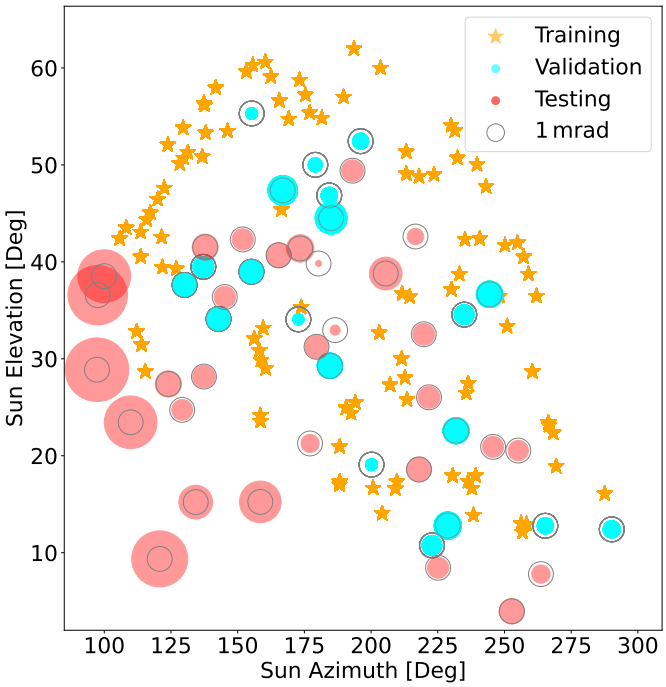

Figure 7: illustration of AJ23 Dataset using 60 Datapoints for training. As it can be seen by the size of the circles, the prediction error inside the distribution in especially small. Only at the edges the accuracy drops slightly.

of the art. It also shows the accuracy of the fine model (neural network) and the hybrid model (prealigned).
All models exhibit similar behavior, with prediction errors decreasing rapidly up to approximately 100 measurements, after which it either plateaus or worsens as more data is added. This behavior is closely related to the distance between the test and training sets, as demonstrated in the lower graph of Fig. 6. Using more than 100 training data points disrupts the balance of the training set, ultimately leading to worse results. We have previously discussed this behavior in more detail in a separate publication (Pargmann et al. (2023)).
The Hybrid-Model achieves the highest accuracies regardless of the size of the data set, and is able to maintain accuracy even in the presence of imbalanced data.
Since the achieved accuracy is highly dependent on the data sets' size, the training/validation/test split and the resulting distribution, we want to present the best achieved results in a transparent representation. This is shown in Figure 7. We chose a representation over the sun angles, as it was found to be the determining factor. The size of the circle in our testing set represents the prediction error and, whereby the circle's radius is adapted linearly, relative to a reference of 1 mrad. To make the plot more readable, a grey circle indicates a prediction error of 1 mrad. The results demonstrate that all data points within the training distribution are accurately predicted, including those at the distribution's edges. Notably, predictions below an elevation of 20° exhibit stable accuracies despite significant extrapolation of over 20° in azimuth and elevation.
For a small statistical assessment, we tested our methodology also with the other data sets. From Fig. 8 it can be concluded that the Hybrid model outperforms the Coarse model, starting from the first measurement except for the AM35 heliostat, which exhibits similar accuracies. However, it should be noted that these results were obtained using an unregularized model, and incorporating weight decay could further enhance the model's performance, which will be investigated in the following.

In order to improve the prediction accuracy of the Hybrid model, we conducted a regularization sweep by gradually reducing the weight decay from Fig. 9a. At a weight decay of 1, the training process will eventually converge to the exact prediction of the coarse model, but better results may be achieved during the convergence process. This explains, why the pretrained fine model's prediction on the validation data still outperforms the coarse model.
When analyzing the test dataset, the model's accuracy remained at the same level as a coarse model (dark and light blue line). This is likely due to the limited size and skewed distribution of our dataset, which results in the model overfitting to the available information and struggling to generalize at the edges of the distribution. The test data set is particularly challenging due to its large dis-

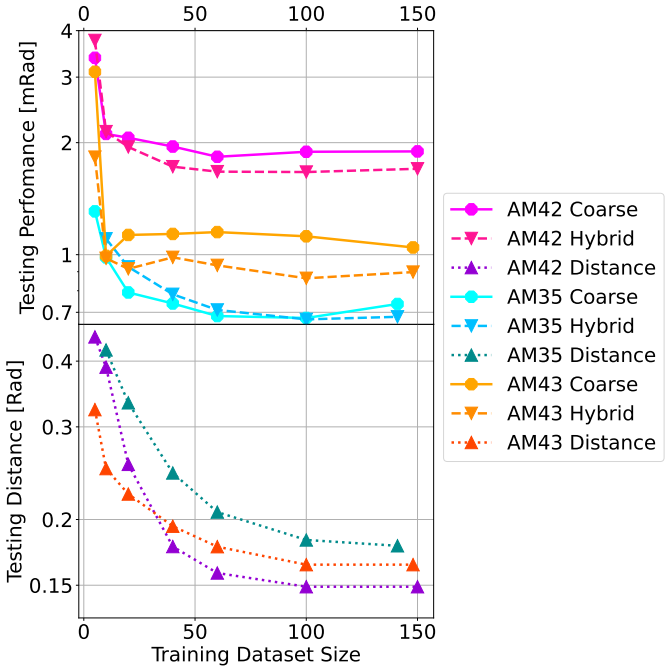

Figure 8: Comparision of our Model to the coarse model with 20 free parameters on different data sets

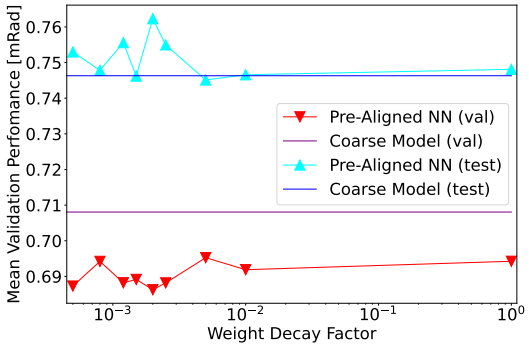

a) Regularization sweep results for the AM35 heliostat.

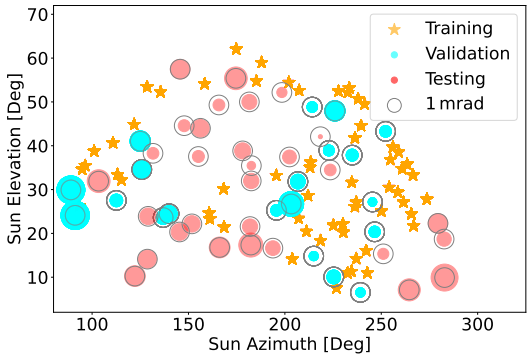

b) Achieved accuracies of the AM35 heliostat on the test and validation data sets using a weight decay factor of 0.0015, which achieved the best validation accuracy.

Figure 9: Results for the AM35 heliostat.

tance from the training dataset. This can be seen in more detail in Fig. 9b.

As expected, errors tend to be higher at the edges of the data distribution. This is seen in both the validation and test dataset where all data points within the data points' distribution's center are predicted better than those at the dataset's edges. Therefore, the average error calculated over the year will likely be smaller than the reported average performance.

Additionally, Fig. 9b demonstrates that the algorithm is capable of high extrapolations over 30 degrees. In summary, even if the test data set performance is only as good as the rigid body model, the overall performance over the year can be judged as superior to the rigid body model, since the model performance only declines at the edges. The accuracy is consistently higher for the inner part of the distribution and thus for the majority of the year.

7. Discussion

Our study demonstrates that our new model outperforms all comparison models. Despite using neural networks, our model provides reliable and traceable behavior of heliostats over the year due to its hybridization with the rigid-body model. However, it is important to consider the data distribution more carefully than with the common approach. The new model has a tendency to produce higher errors in edge regions due to the significantly increased number of free parameters in those regions. While this may not significantly impact the annual average, it can result in higher errors during early morning and late evening hours. Moreover, this issue can be easily addressed through targeted measurements in the morning and evening.

The data set obtained from AM43 exhibited the highest level of accuracy using the Hybrid model, albeit with the smallest improvement when compared to the Coarse model. This could potentially be attributed to the impact of measurement errors, which become increasingly significant at higher levels of accuracy. At the solar tower in Jülich, the vectorial deviation between model an reality is determined by calculating the centroid of area of each focal spot, which is then compared to the target point. However, various factors such as mirror deformations, over/underexposure, partial shading by heliostats located in front, and algorithmic instabilities can result in inaccuracies in the measurement. To further minimize these errors, it may be useful to calculate the loss directly from the recorded image instead of the vectorial deviation. For example, this can be achieved through the use of a differentiable ray tracing environment (Pargmann et al. (2023)).

In future works, model architecture investigations could improve model prediction capabilities even further.

8. Conclusion

In this study, we proposed a Hybrid-Model that combines a coarse rigid body model with a fine neural network model to predict the motor positions for heliostats in the solar power plant in Jülich. Using this technique, we achieved higher accuracies than all tested rigid body models, independent of the data set size. The results demonstrate that all data points within the test/validation data sets are accurately predicted, including those at the distribution's edges. Simultaneously we lowered the amount of data compared to previously full deep learning models by a factor of 5 for reaching top accuracies below 0.7 mrad and is able to maintain accuracy even in the presence of imbalanced data. The reported accuracies exhibit large distances to the training data set over 20 degrees. Overall, our study contributes to the development of more accurate and reliable solar power plant operations.

Competing interests

The authors declare no competing interests.

References

K. W. Stone, Automatic heliostat track alignment method, 1986. US Patent 4,564,275.

M. P. Sarr, A. Thiam, B. Dieng, ANFIS and ANN models to predict heliostat tracking errors, Heliyon 9 (2023) e12804. URL: https://www.sciencedirect.com/science/article/pii/S2405844023000117. doi:10.1016/j.heliyon.2023.e12804.

M. Pargmann, D. Maldonado Quinto, P. Schwarzbözl, R. Pitz-Paal, High accuracy data-driven heliostat calibration and state prediction with pretrained deep neural networks, Solar Energy 218 (2021) 48–56. URL: https://www.sciencedirect.com/science/article/pii/S0038092X21000621. doi:10.1016/j.solener.2021.01.046.

R. Baheti, P. Scott, Design of self-calibrating controllers for heliostats in a solar power plant, IEEE Transactions on Automatic Control 25 (1980) 1091–1097. URL: http://ieeexplore.ieee.org/document/1102527/. doi:10.1109/TAC.1980.1102527.

K. W. Stone, Automatic heliostat track alignment method, 1986. URL: https://patents.google.com/patent/US4564275A/en.

Y. T. Chen, A. Kribus, B. H. Lim, C. S. Lim, K. K. Chong, J. Karni, R. Buck, A. Pfahl, T. P. Bligh, Comparison of Two Sun Tracking Methods in the Application of a Heliostat Field, Journal of Solar Energy Engineering 126 (2004) 638–644. URL: https://asmedigitalcollection.asme.org/solarenergyengineering/article/126/1/638/451491/Comparison-of-Two-Sun-Tracking-Methods-in-the. doi:10.1115/1.1634583.

Y. T. Chen, B. H. Lim, C. S. Lim, General Sun Tracking Formula for Heliostats With Arbitrarily Oriented Axes, Journal of Solar Energy Engineering 128 (2006) 245–250. URL: https://asmedigitalcollection.asme.org/solarenergyengineering/article/128/2/245/478177/General-Sun-Tracking-Formula-for-Heliostats-With. doi:10.1115/1.2189868.

K.-K. Chong, C.-W. Wong, F.-L. Siaw, T.-K. Yew, S.-S. Ng, M.-S. Liang, Y.-S. Lim, S.-L. Lau, Integration of an On-Axis General Sun-Tracking Formula in the Algorithm of an Open-Loop Sun-Tracking System, Sensors 9 (2009) 7849–7865. URL: http://www.mdpi.com/1424-8220/9/10/7849. doi:10.3390/s91007849.

M. Guo, Z. Wang, W. Liang, X. Zhang, C. Zang, Z. Lu, X. Wei, Tracking formulas and strategies for a receiver oriented dual-axis tracking toroidal heliostat, Solar Energy 84 (2010) 939–947. URL: https://linkinghub.elsevier.com/retrieve/pii/S0038092X10001052. doi:10.1016/j.solener.2010.02.015.

S. S. S. Khalsa, C. K. Ho, C. E. Andraka, AN AUTOMATED METHOD TO CORRECT HELIOSTAT TRACKING ERRORS (2010) 10.

M. Guo, F. Sun, Z. Wang, J. Zhang, Properties of a general azimuth–elevation tracking angle formula for a heliostat with a mirror-pivot offset and other angular errors, Solar Energy 96 (2013) 159–167. URL: https://linkinghub.elsevier.com/retrieve/pii/S0038092X13002612. doi:10.1016/j.solener.2013.06.031.

E. Smith, C. Ho, Field Demonstration of an Automated Heliostat Tracking Correction Method, Energy Procedia 49 (2014) 2201–2210. URL: https://linkinghub.elsevier.com/retrieve/pii/S1876610214006870. doi:10.1016/j.egypro.2014.03.233.

J. Freeman, B. Shankar, G. Sundaram, Inverse kinematics of a dual linear actuator pitch/roll heliostat, AIP Conference Proceedings 1850 (2017) 030018. URL: https://aip.scitation.org/doi/abs/10.1063/1.4984361. doi:10.1063/1.4984361, publisher: American Institute of Physics.

V. Grigoriev, K. Milidonis, M. Blanco, Sun tracking by heliostats with arbitrary orientation of primary and secondary axes, Solar Energy 207 (2020) 1384–1389. URL: https://linkinghub.elsevier.com/retrieve/pii/S0038092X20308185. doi:10.1016/j.solener.2020.07.086.

V. Grigoriev, K. Milidonis, M. Blanco, M. Constantinou, Method to determine the tracking angles of heliostats, MethodsX 8 (2021) 101244. URL: https://www.sciencedirect.com/science/article/pii/S2215016121000376. doi:10.1016/j.mex.2021.101244.

S.-E. Lee, Y.-C. Park, Modeling of Heliostat Sun Tracking Error Using Multilayered Neural Network Trained by the Extended Kalman Filter, Journal of Institute of Control, Robotics and Systems 16 (2010) 711–719. URL: https://koreascience.kr/article/JAKO201027042827853.page. doi:10.5302/J.ICROS.2010.16.7.711, publisher: Institute of Control, Robotics and Systems.

L. Guangyu, C. Zhongkun, Heliostat attitude angle detection method based on BP neural network, MATEC Web of Conferences 139 (2017) 00043. URL: https://www.matec-conferences.org/articles/matecconf/abs/2017/53/matecconf_icmite2017_00043/matecconf_icmite2017_00043.html. doi:10.1051/matecconf/201713900043, publisher: EDP Sciences.

N. AL-Rousan, N. A. Mat Isa, M. K. Mat Desa, Efficient single and dual axis solar tracking system controllers based on adaptive neural fuzzy inference system, Journal of King Saud University - Engineering Sciences 32 (2020) 459–469. URL: https://www.sciencedirect.com/science/article/pii/S1018363920302233. doi:10.1016/j.jksues.2020.04.004.

M. Pargmann, M. Leibauer, V. Nettelroth, D. Maldonado Quinto, R. Pitz-Paal, It is Not About Time - A New Standard for Open-Loop Heliostat Calibration Methods, preprint, In Review, 2023. URL: https://www.researchsquare.com/article/rs-2898838/v1. doi:10.21203/rs.3.rs-2898838/v1.

M. Tancik, P. Srinivasan, B. Mildenhall, S. Fridovich-Keil, N. Raghavan, U. Singhal, R. Ramamoorthi, J. Barron, R. Ng, Fourier features let networks learn high frequency functions in low dimensional domains, Advances in Neural Information Processing Systems 33 (2020) 7537–7547.

M. Pargmann, J. Ebert, D. M. Quinto, R. Pitz-Paal, S. Kesselheim, In-Situ Solar Tower Power Plant Optimization byDifferentiable Ray Tracing, preprint, In Review, 2023. URL: https://www.researchsquare.com/article/rs-2554998/v1. doi:10.21203/rs.3.rs-2554998/v1.